



LAWRENCE  
LIVERMORE  
NATIONAL  
LABORATORY

# Microscopic mechanisms of equilibrium melting of a solid

A. Samanta, E. Weinan, T. Yu, M. Tuckerman

July 14, 2014

Science

## **Disclaimer**

---

This document was prepared as an account of work sponsored by an agency of the United States government. Neither the United States government nor Lawrence Livermore National Security, LLC, nor any of their employees makes any warranty, expressed or implied, or assumes any legal liability or responsibility for the accuracy, completeness, or usefulness of any information, apparatus, product, or process disclosed, or represents that its use would not infringe privately owned rights. Reference herein to any specific commercial product, process, or service by trade name, trademark, manufacturer, or otherwise does not necessarily constitute or imply its endorsement, recommendation, or favoring by the United States government or Lawrence Livermore National Security, LLC. The views and opinions of authors expressed herein do not necessarily state or reflect those of the United States government or Lawrence Livermore National Security, LLC, and shall not be used for advertising or product endorsement purposes.

# Microscopic mechanisms of equilibrium melting of a solid

Amit Samanta\*

*Program in Applied and Computational Mathematics,  
Princeton University, Princeton, New Jersey 08544, USA  
and Condensed Matter and Materials Division,  
Lawrence Livermore National Laboratory, Livermore, CA 94550 USA*

Weinan E<sup>†</sup>

*BICMR and School of Mathematical Sciences, Peking University, Beijing, China  
and Department of Mathematics and Program in Applied and Computational Mathematics,  
Princeton University, Princeton, New Jersey 08544, USA*

Tang-Qing Yu

*Courant Institute of Mathematical Sciences,  
New York University, New York 10012, USA*

Mark E. Tuckerman<sup>‡</sup>

*Department of Chemistry and Courant Institute of Mathematical Sciences,  
New York University, New York 10003, USA*

(Dated: July 11, 2014)

## Abstract

**Melting of a solid, like other first-order phase transitions, exhibits an intrinsic time-scale disparity – the time spent by the system in metastable states is orders of magnitude longer than the transition times between the states. Thus, elucidating the mechanism of melting has proved challenging. Using robust rare-event sampling techniques, we find that melting in copper and aluminum can occur via multiple, competing pathways involving the formation of point defects or dislocations. Each path is characterized by multiple barrier crossing events arising from multiple metastable states within the solid basin. With increase in temperature melting mechanisms change from a multiple free energy barrier crossing event to a single barrier crossing event at superheated conditions and to a vibrational instability at the limit of super heating.**

Theoretical work on the melting of a solid dates back to Lindemann who in 1910 envisioned the melting transition as a vibrational instability.<sup>1</sup> Later, in 1939, Born postulated the macroscopic instability criteria of a solid in terms of the elastic constants.<sup>2-4</sup> Most other theoretical models are centered around the role of defects – point defects such as vacancies, interstitials and line defects such as dislocations – that proliferate in the solid close to the melting point.<sup>5-9</sup>

Contrary to these melting theories, classical notions of homogeneous melting envision the formation of an initial liquid nucleus that is aided by thermal fluctuations without any preferential nucleating sites.<sup>10,11</sup> Within the framework of the classical nucleation theory (CNT), the radius  $r$  of the liquid nucleus serves as a reaction coordinate, and the Gibbs free energy  $\Delta G(r)$  is a balance between the free energy gained in forming a liquid nucleus of volume  $4\pi r^3/3$  and the work needed to create an interface between the solid and such a nucleus

$$\Delta G(r) = \frac{4}{3}\pi r^3 \rho \Delta\mu + 4\pi r^2 \gamma_s. \quad (1)$$

Here  $\Delta\mu = \mu_l - \mu_s < 0$  is the chemical potential difference between the liquid and solid phases,  $\rho$  is the liquid density,  $4\pi r^2$  is the surface area of the nucleus, and  $\gamma_s$  is its surface tension. The critical nucleus size  $r^* = -2\gamma_s/(\rho\Delta\mu)$  maximizes this free energy<sup>12</sup> ( $\Delta G(r^*) = 16\pi\gamma_s^3/3(\rho\Delta\mu)^2$ ) and determines the length scale beyond which growth of the cluster becomes favorable. At the solid-liquid coexistence point,  $\Delta\mu = 0$ , and the theory predicts an infinite free energy barrier and corresponding suppression of the nucleation rate. This picture involves numerous simplifying assumptions and fails to account for the potentially important role of defects, dislocations, and multiple barriers along potential melting paths.<sup>12</sup>

Close to the coexistence point, the melting of a solid involves activation from a metastable local minimum. Consequently, a theoretical analysis of the melting mechanisms close to the thermodynamic melting point using standard atomistic simulation methods is not feasible because melting is a rare barrier-crossing event with mean first passage time many orders of magnitude greater than the vibrational frequency of atoms. State-of-the-art rare-event sampling techniques now render possible the computational study of equilibrium melting and the extraction of dominant pathways and free energetics. We employ adiabatic free energy dynamics (AFED),<sup>13-16</sup> together with the string method<sup>17,18</sup> in order to explore the multidimensional free energy surface (FES) efficiently and to construct a microscopic picture of the melting process for two commonly studied prototypical systems: copper and aluminum.<sup>19,20</sup>

We begin by analyzing the equilibrium melting process using as collective variables the volume ( $V$ ) of the system and the two Steinhardt order parameters  $Q_4$  and  $Q_6$  (see the Supplementary Information (SI) for details) - together they capture the orientational and positional ordering. In Figs. 1(a) and 1(b), we show a projection of the Gibbs FES onto the  $V$ - $Q_4$  subspace for Cu at 1350 K and 1 atm pressure. Contrary to the simple picture from CNT of a smooth FES possessing metastable solid and liquid basins separated by an index-1 saddle point, the FES obtained here has multiple locally stable states characterized by different defects, mainly vacancy-interstitial pairs, dislocations, and interstitial clusters, and the free energy barriers separating these states exhibit multiple scales. The FES for Al at the melting point (Fig. S2) exhibits a similar structure. Figure 1(c) illustrates how vacancy-interstitial pairs can form, diffuse, cluster, and annihilate.

The existence of a multitude of metastable states suggests that there exists an ensemble of multiple competing transition pathways. One such melting channel and the associated free energy profile is shown in Fig. 2(a). Along this path, as the system moves out of the solid basin, the volume of the solid and the number of vacancy and interstitial pairs increases. Thus, this particular melting pathway proceeds via the formation of point defects, which is entropically favorable but energetically costly. The competition between entropic and enthalpic contributions causes the free energy to reach a maximum value (marked S2 in Fig. 2(a)) at a certain defect concentration. After the saddle S2, the system lowers its free energy by forming defect clusters at the expense of isolated defects. Cluster formation is enabled via the defect kinetics. In both copper and aluminum, diffusion barriers of interstitial defects are quite small (0.08 eV and 0.13 eV, respectively); barriers for vacancy diffusion somewhat larger (0.8 eV and 0.65 eV, respectively). Previously, Couchman and Reynolds had conjectured a relationship between the melting point and vacancy concentration thus suggesting a direct role of vacancy diffusion in the melting process<sup>21</sup>. At 1350 K in Cu, these defects are mobile and diffuse over long distances in the solid. Occasionally, some of these interstitial and vacancy migration paths meet, and defect clusters can form. Inside these defect clusters, there is a significant loss of crystalline order (the local Steinhardt parameter  $\bar{q}_6 \sim 0.1$ ), which coincides with an enhanced diffusivity of atoms inside the cluster. After S2, the system moves to a shallow metastable state, and the defect cluster evolves into a liquid nucleus, the existence of which during melting also constitutes a deviation from the CNT.

As the system moves out of the metastable state towards the saddle S1, the size of the liquid nucleus increases. This process is sometimes observed to be aided by the coalescence of a few smaller liquid nuclei. After the liquid nucleus attains a critical size, the free energy along the path

decreases. This corresponds to the second important bottleneck with a barrier of  $\sim 3.75$  meV/atom relative to the solid basin and  $\sim 20$  eV relative to the metastable state in the melting transition. From here, the liquid nucleus simply increases in size until the entire system transforms to the liquid state.

Our enhanced sampling calculations suggest the existence of a melting path along which dislocation activity aids the formation of an initial liquid nucleus. The corresponding free energy profile and key saddle structures are shown in Fig. 2(b). Along this path, we first observe the formation of defect clusters from point defects followed by the heterogeneous nucleation of dislocations from the defect clusters. The dislocation density increases as the system moves towards the saddle S1 and the first liquid embryo is formed heterogeneously from these dislocations. This process of initiating melting from dislocations is reminiscent of recent observations of heterogeneous nucleation in colloidal systems<sup>22</sup> and embedded Pb nanoparticles in an Al matrix<sup>7</sup> and differs significantly from the notion of proliferation of dislocations.<sup>6,8</sup>

From our analysis of the escape pathways from the solid basin, we conclude that melting has a high probability of being coupled to defect activity. Nevertheless, motivated by recent reports of melting without the aid of defects,<sup>23</sup> we were inspired to ask if it is possible for melting to occur in this manner. By calculating Voronoi volumes associated with each of the atoms, we were able to show that, close to the melting point, the free volume associated with vacancies is spatially delocalized, and it is difficult to identify individual defects. As previous experiments have shown, on-the-fly determination of defects at high temperatures is nontrivial.<sup>24</sup> Furthermore, under equilibrium conditions, the possibility that a system exists without defects at 1350 K in Cu seems remote because of the presence of nearly degenerate defect states with transition barriers on the order of 1-2 eV. Nevertheless, we explored the possibility of a melting pathway connecting the defect-free solid minimum and the liquid basin that does not pass through the defect states. On the FES, a possible pathway for melting without the aid of defects has a notably higher free energy barrier ( $\sim 4.13$  meV/atom) than the barriers along the defect mediated melting pathways. Along such a defect-free path, the formation of the initial liquid nucleus is correlated with thermal fluctuations and is not aided by any stable defects. However, if this path is allowed to relax in path space, it eventually converges to one of the two defect mediated melting pathways.

Temperature plays an important role in determining the characteristics of the FES. Thus, we also sought to compare equilibrium melting to melting of a superheated solid. As the system is superheated beyond the melting point, the liquid basin engulfs larger portions of the FES, and

the metastable state without any defects vanishes (Fig. 1(*d*)). This change in the FES affects the melting mechanisms: compared to the FES at 1350 K in Cu, at 1550 K there are fewer locally stable states present inside the solid basin, and there is only one important bottleneck for melting, namely, the barrier to escape the solid basin. Interestingly, this barrier has a significant entropic contribution (Fig. S4). The absence of metastable state without defects indicates that melting at these superheated conditions always originates from a solid with pre-existing point defects or defect clusters.

With further increase in temperature, the melting barrier along the minimum free energy path vanishes at  $\sim 1600$  K in Cu and  $\sim 1275$  K in Al. Above these temperatures, atoms execute large-amplitude vibrations about their equilibrium positions, and the solid to liquid transition is a consequence of an instability (inset in Fig. 2(*c*)). The crucial role of the vibrational amplitude in this process is realized only by separating the diffusive motions of the atoms from their vibrational motions. This mechanism is reminiscent of Lindemann’s vibrational instability<sup>1</sup> and is in agreement with recent experimental observations of melting in superheated aluminum.<sup>25</sup> The fact that Lindemann’s criterion corresponds to an instability of the solid and not to equilibrium melting leads to an overestimation of the melting point. This is relevant because Lindemann’s criterion is still commonly used to determine the melting point of a solid.<sup>26–29</sup>

The presence of regions that lack proper orientational and translational ordering, which include defect clusters, voids, grain boundaries, and dislocations increases the energy of a solid and lead to heterogeneous melting. We sought to investigate this case by initiating trajectories from pre-existing dislocations and from grain boundaries obtained by rapidly cooling the liquid. In both cases, the resulting metastable states lie closer to the saddle S1 on the FES, resulting in a decrease in the melting barrier. As shown in Fig. 2(*d*), melting in a solid with grain boundaries is initiated at these boundaries, and the barrier can be as low as 6 eV at the melting point (Fig. S8). The atoms in the grain boundaries are fluid-like and melting happens by gradual growth of these liquid-like region. In a solid with multiple dislocations, the elastic interactions between the dislocations can decrease the melting barrier by as much as a factor of six below the  $\sim 120$  eV barrier for melting of a copper sample without any pre-existing defects. More details of these studies are provided in the Supporting Information.

Fig. 2(*c*) shows the sensitivity of the free energy surface to temperature. There exist three different melting regimes: (i) close to the melting point (i.e.  $T < 1525$  K for Cu), the transition occurs via multiple barrier crossings, and elastic interactions play a dominant role in determining

the melting mechanisms; (ii) at superheated temperatures (i.e. 1525 K to 1590 K for Cu), the solid to liquid transition is a single barrier crossing event, and melting can be understood in terms of the classical notion of competition between surface and bulk energy contributions; (iii) at the limit of instability, melting is initiated by the propagation of large vibrations of the atoms in a short span of time across the crystal. This large variation in the underlying melting mechanisms suggests a strong coupling between the orientational order, density, and temperature: at a given temperature, how  $Q_6$  and  $Q_4$  change with  $V$  determines the structure of defects present in the solid, locations of the saddle points, and the basins of attraction.

Notwithstanding the above differences in the melting mechanisms, we find that melting is aided by mobile defects at both the thermodynamic melting and conditions of superheating. In both of these states, defects constitute less than  $10^{-3}$  of the total lattice sites. Consequently, melting and lattice instabilities are not triggered by the proliferation of defects,<sup>7,30–32</sup> which contrasts with theories based on the assertion that “melting is correlated with the achievement of a critical vacancy concentration”.<sup>33</sup> Further, our enhanced sampling calculations reveal that the size of a liquid nucleus does not change smoothly along the minimum free energy pathway.

Fig. 3 compares our findings to the picture suggested by CNT. It is clear that multiple, competing pathways and multiple barrier crossing events along each path are crucial for the formation of the initial liquid embryo and constitute a qualitative departure from the simplifying assumptions of CNT. An important element that is clearly missing in the  $\Delta G$  of CNT is the contribution from the strain energy. Along the dislocation mediated melting pathway (Fig. 2(b)), for example, the liquid nucleus is formed preferentially on the dislocations via a decrease in the strain energy associated with the dislocations. The change in free energy can be expressed as  $\Delta G(r) = -\alpha r \log r/r_o + \Delta\mu 4\pi r^3/3 + 4\pi r^2 \gamma_s$ , where  $\alpha = Gb^2/4\pi(1-\nu)$ ,  $r_o$  is a constant, and  $-\alpha r \log r/r_o$  is the decrease in the elastic energy of the dislocation due to the formation of the liquid nucleus.<sup>34</sup> At the melting point  $\Delta\mu = 0$ , hence the critical radius of the liquid nucleus is  $r^* \sim Gb^2/32\pi^2\gamma_s(1-\nu)$ . Similarly, formation of dislocations from point defects and defect clusters involves a competition between the elastic energy of dislocation and the interaction energy between the dislocation and the defects, likely requiring the addition of non-local energy terms in any mean-field type of description of melting. This physical interplay of processes with multiple length and time-scales indicates that melting of a solid cannot be viewed through the simple lens of CNT but should be regarded as a complex “multi-scale” phenomenon.



- 
- \* Electronic address: `asamanta@math.princeton.edu`
- † Electronic address: `weinan@math.princeton.edu`
- ‡ Electronic address: `mark.tuckerman@nyu.edu`
- <sup>1</sup> F. A. Lindemann, *Physikalische Zeitschrift* **11**, 609 (1910).
- <sup>2</sup> M. Born, *Journal of Chemical Physics* **7**, 591 (1939).
- <sup>3</sup> N. F. Mott, *Nature* **145**, 801 (1940).
- <sup>4</sup> J. L. Tallon, *Nature* **299**, 188 (1982).
- <sup>5</sup> N. F. Mott, *Proceedings of the Royal Society of London. Series A. Mathematical and Physical Sciences* **215**, 1 (1952).
- <sup>6</sup> D. Kuhlmann-Wilsdorf, *Physical Review* **140**, A1599 (1965).
- <sup>7</sup> T. Gorecki, *Zeitschrift fuer Metallkunde/Materials Research and Advanced Techniques* **65**, 426 (1974).
- <sup>8</sup> L. Gómez, A. Dobry, C. Geuting, H. T. Diep, and L. Burakovsky, *Physical Review Letters* **90**, 095701 (2003).
- <sup>9</sup> X. M. Bai and M. Li, *Physical Review B* **77**, 134109 (2008).
- <sup>10</sup> M. Volmer and A. Weber, *Z. Physik. Chem.* **119**, 277 (1926).
- <sup>11</sup> R. Becker and W. Doering, *Annalen der Physik* **24**, 719 (1935).
- <sup>12</sup> R. P. Sear, *International Materials Reviews* **57**, 328 (2012).
- <sup>13</sup> L. Rosso, P. Mináry, Z. Zhu, and M. E. Tuckerman, *Journal of Chemical Physics* **116**, 4389 (2002).
- <sup>14</sup> L. Maragliano and E. Vanden-Eijnden, *Chemical Physics Letters* **426**, 168 (2006).
- <sup>15</sup> J. B. Abrams and M. E. Tuckerman, *Journal of Physical Chemistry B* **112**, 15742 (2008).
- <sup>16</sup> T. Q. Yu and M. E. Tuckerman, *Physical Review Letters* **107**, 015701 (2011).
- <sup>17</sup> W. E, W. Ren, and E. Vanden-Eijnden, *Journal of Physical Chemistry B* **109**, 6688 (2005).
- <sup>18</sup> L. Maragliano, A. Fischer, E. Vanden-Eijnden, and G. Ciccotti, *Journal of Chemical Physics* **125**, 024106 (2006).
- <sup>19</sup> R. Lynden-Bell, J. Van Duijneveldt, and D. Frenkel, *Molecular Physics* **80**, 801 (1993).
- <sup>20</sup> M. Forsblom and G. Grimvall, *Nature Materials* **4**, 388 (2005).
- <sup>21</sup> P. R. Couchman and C. L. Reynolds, *Philosophical Magazine* **34**, 327 (1976).
- <sup>22</sup> A. M. Alsayed, M. F. Islam, J. Zhang, P. J. Collings, and A. G. Yodh, *Science* **309**, 1207 (2005).
- <sup>23</sup> Z. Wang, F. Wang, Y. Peng, Z. Zheng, and Y. Han, *Science* **338**, 87 (2012).

- <sup>24</sup> E. Fukushima and A. Ookawa, Journal of the Physical Society of Japan **10**, 970 (1955).
- <sup>25</sup> B. J. Siwick, J. R. Dwyer, R. E. Jordan, and R. J. D. Miller, Science **302**, 1382 (2003).
- <sup>26</sup> J. J. Gilvarry, Physical Review **102**, 308 (1956).
- <sup>27</sup> Z. H. Jin, P. Gumbsch, K. Lu, and E. Ma, Physical Review Letters **87**, 055703 (2001).
- <sup>28</sup> K. Sokolowski-Tinten, C. Blome, J. Blums, A. Cavalleri, C. Dietrich, A. Tarasevitch, T. Uschmann, E. Forster, M. Kammler, M. Horn-von Hoegen, et al., Nature **422**, 287 (2003).
- <sup>29</sup> M. Martinez-Canales, C. J. Pickard, and R. J. Needs, Physical Review Letters **108**, 045704 (2012).
- <sup>30</sup> R. W. Cahn, Nature **273**, 491 (1978).
- <sup>31</sup> R. M. J. Cotterill and J. U. Madsen, Nature **288**, 467 (1980).
- <sup>32</sup> H. J. Fecht and W. L. Johnson, Nature **334**, 50 (1988).
- <sup>33</sup> R. W. Cahn, Nature **334**, 17 (1988).
- <sup>34</sup> J. W. Cahn, Acta Metallurgica **5**, 169 (1957).
- <sup>35</sup> B. J. Alder, W. G. Hoover, and T. E. Wainwright, Physical Review Letters **11**, 241 (1963).
- <sup>36</sup> D. Gebauer, A. Vliet, and H. Clfen, Science **322**, 1819 (2008).

**Acknowledgements** W. E and A. S. acknowledge support by ONR (N00014-13-1-0338), ARO (Grant No. W911NF-11-1-0101), DOE (Grant No. DE-SC0009248). M.E.T. acknowledges support from NSF grant CHE-1301314. A.S is supported by the DOE at the Lawrence Livermore National Laboratory under Contract DE-AC52-07NA27344.

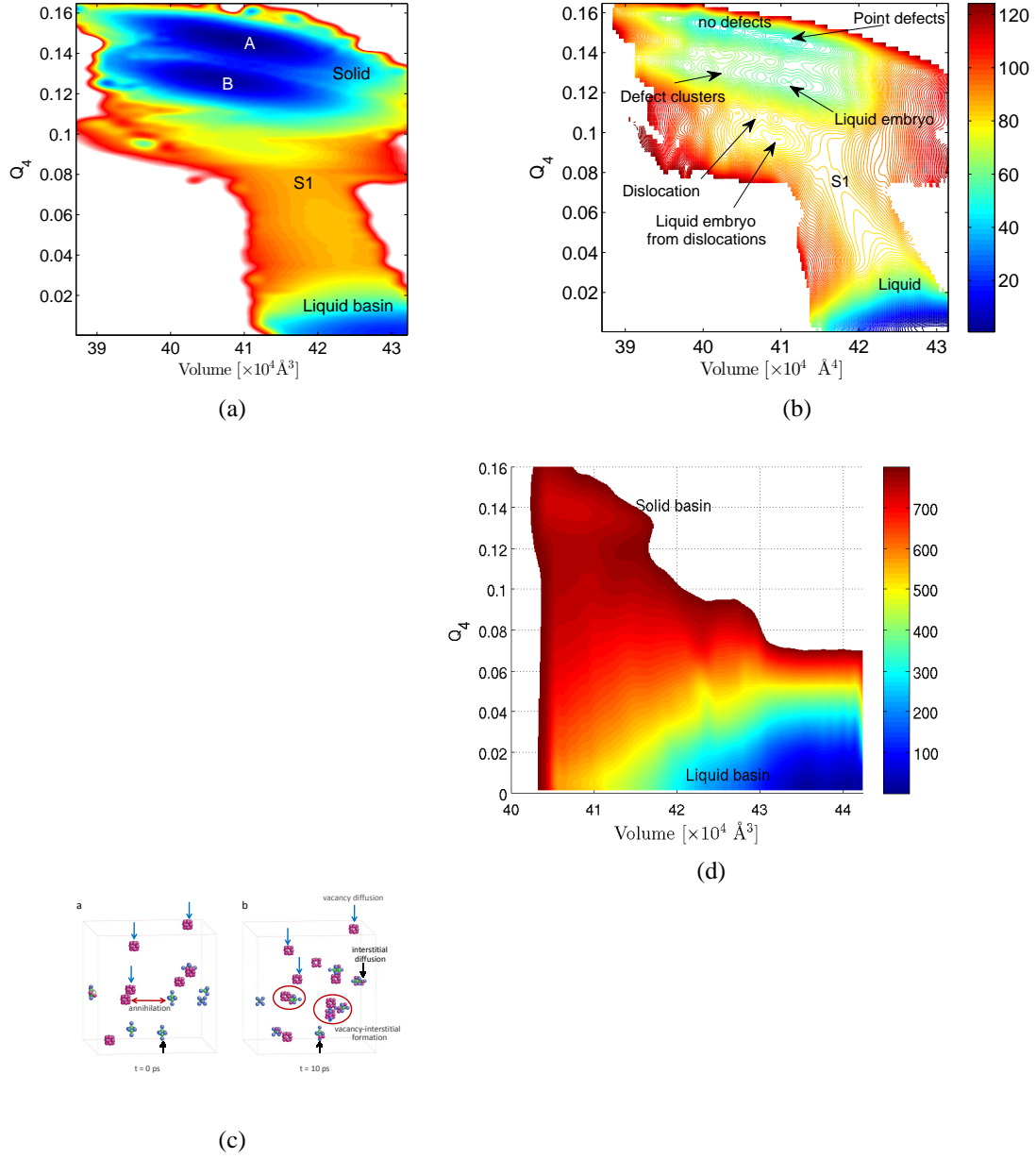


FIG. 1: The FES of a solid shows multi-scale characteristics and is sensitive to temperature. Shown here are the FESs at 1350 K and 1 atm for Cu, in panels (a) and (b), and at 1550 K in panel (c). The solid basin at 1350 K contains two valleys (marked A and B in 1(a)) separated by a shallow ridge. Valley A contains local minima pertaining to the solid with or without point defects, while Valley B contains local minima pertaining mainly to defect clusters. Within valley A, atomic motions in the state without defects are highly correlated<sup>9,35</sup>) and have a waiting time of  $\sim 500 \text{ ps}$  while point-defect related diffusive motions of atoms have a waiting time of  $\sim 10 \text{ ps}$  (Fig. S3). Inside valley B, as the volume of the system increases, the defect cluster develops liquid like characteristics. A time evolution of defects in the solid basin is shown in panel (c). The dominant atomic processes are vacancy-interstitial formation, vacancy diffusion (highlighted by blue arrows), interstitial diffusion (black arrows), interstitial cluster formation, vacancy-interstitial annihilation (red double ended arrow). Processes such as vacancy-interstitial pair formation and vacancies and interstitials forming clusters are circled in red. The FES at 1550 K, in panel (d), illustrates how the melting mechanisms changes from to a single barrier crossing event at superheated conditions

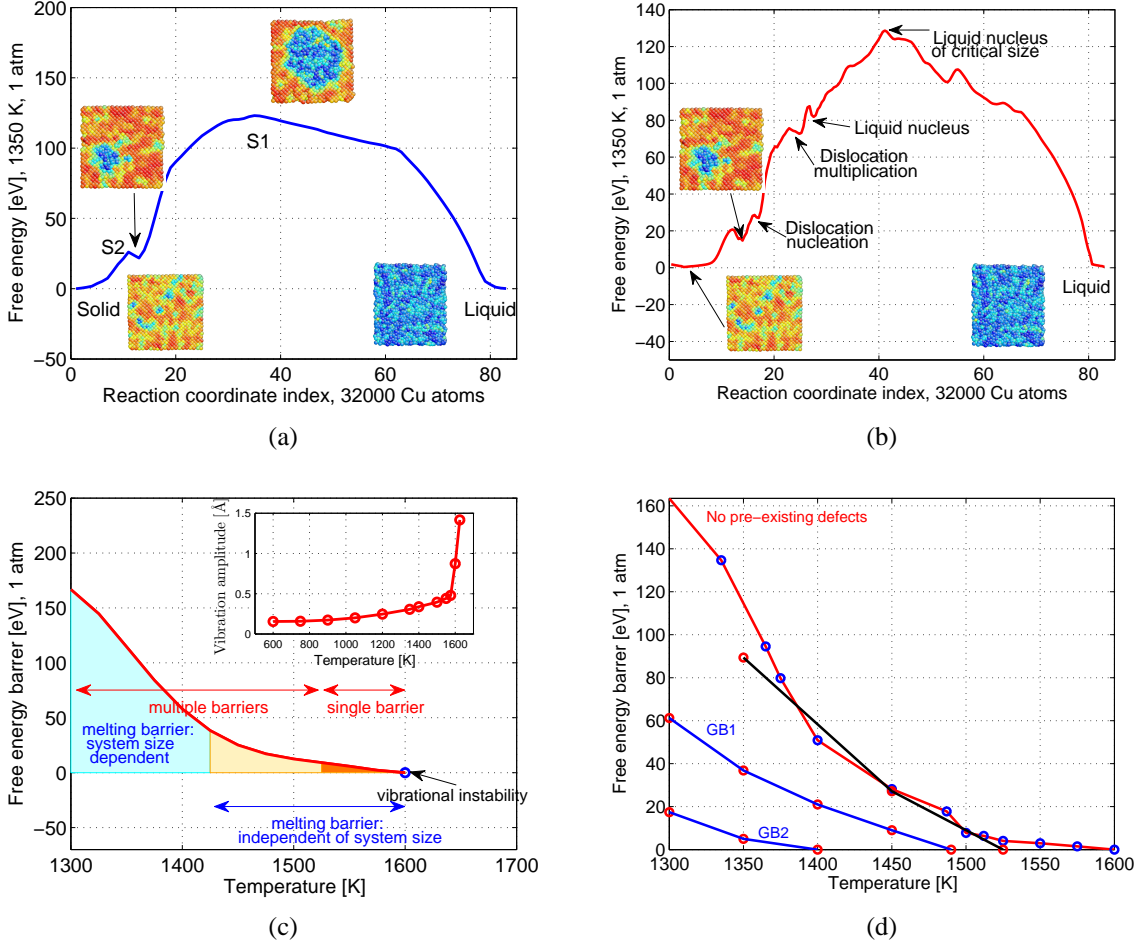


FIG. 2: Melting in a solid without pre-existing defects can proceed via multiple competing pathways as shown in panels (a) and (b) for Cu at 1350 K. Along the point defect mediated melting pathway (2(a)), there are two important saddles: S2 (formation of defect cluster) and S1 (formation of liquid nucleus of critical size). Along the dislocation mediated melting pathway in 2(b), there are multiple barriers including defect cluster formation, dislocation nucleation, liquid nucleus formation, etc. The atoms are colored according to the local orientation order parameter  $\bar{q}_4$ . The inset in panel (c) shows the sharp discontinuity in the vibrational amplitude ( $a_v$ ) of atoms vibrating about their mean positions in the solid local basin, which coincides with the vanishing of the free energy barrier.  $a_v$  is extracted from the root-mean-squared-displacement (rmsd) after subtracting the diffusion contributions and hence the sharp discontinuity observed in  $a_v$  is not observed in the usual rmsd profiles as a function of the temperature. (for example Fig 2 in Ref. 27). The effect of grain boundaries, dislocations on the melting barriers are shown in panel (d). The solid in GB1 has only two grains while GB2 has about 4 grains.

## Melting of an ideal lattice at melting point

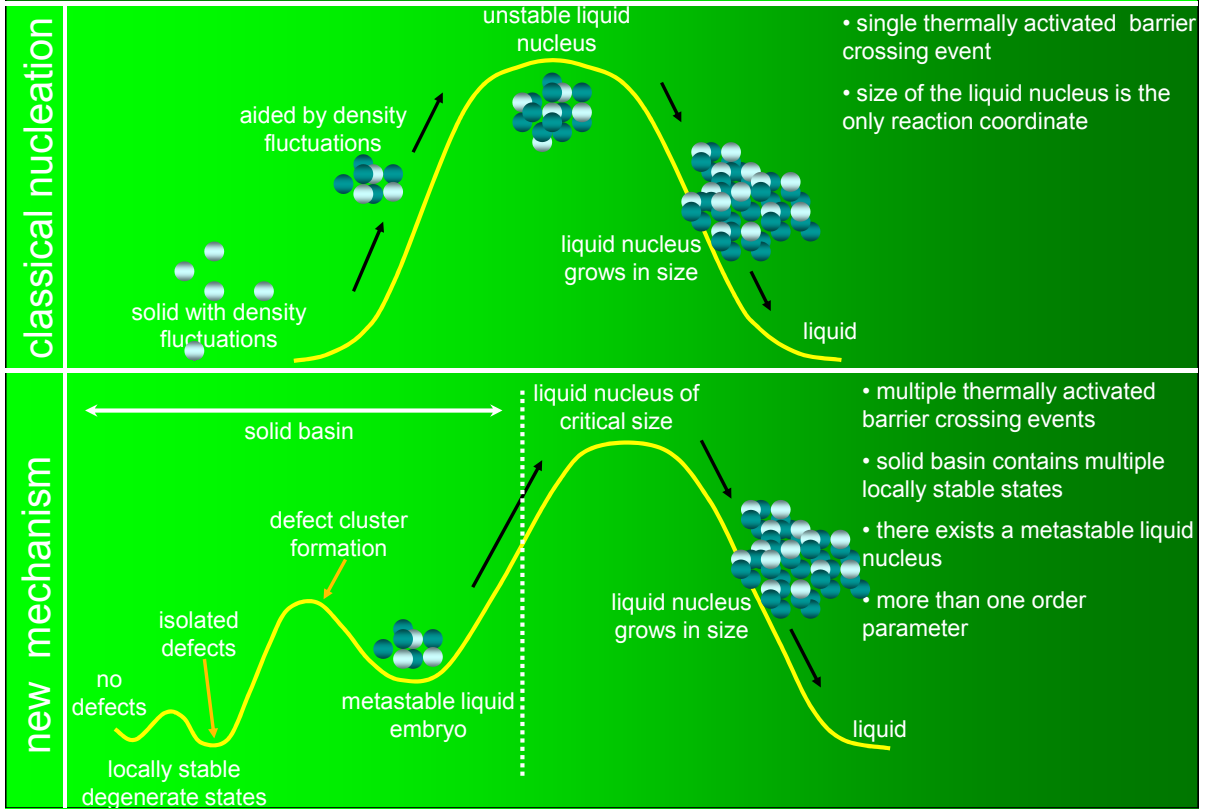


FIG. 3: An illustration of the CNT and the melting mechanisms observed in our simulations. The barrier to melting in the new, proposed mechanism is smaller than the homogeneous melting scenario. Recent experiments point to the existence of stable prenucleation clusters during the initial stages of crystallization<sup>36</sup>. Thus, it is plausible that there exist multiple metastable states in the liquid basin as well.